Published in final edited form as:
Ophthalmology. 2009 December ; 116(12): 2448–2456. doi:10.1016/j.ophtha.2009.06.003.

Insights into Advanced Retinopathy of Prematurity Using Handheld Spectral Domain Optical Coherence Tomography Imaging

Sai H. Chavala, MD, **Sina Farsiu, PhD**, **Ramiro Maldonado, MD**, **David K. Wallace, MD**, **Sharon F. Freedman, MD**, and **Cynthia A. Toth, MD**
Department of Ophthalmology, Duke University Medical Center, Duke University, Durham, North Carolina

Abstract

Purpose—To elucidate the subclinical anatomy of retinopathy of prematurity (ROP) using spectral domain optical coherence tomography (SD OCT).

Design—Prospective, observational case series.

Participants—Three low-birth-weight, severely premature infants.

Methods—Clinical examination was performed using a portable slit lamp and indirect ophthalmoscope. Imaging was performed by using a handheld SD OCT device and Retcam (Clarity Medical Systems, Pleasanton, CA) or video-indirect recording. Spectral domain optical coherence tomography imaging was conducted without sedation at the bedside in the neonatal intensive care unit on 1 patient. The other 2 patients had an examination under anesthesia with SD OCT imaging in the operating room.

Main Outcome Measures—In vivo determination of vitreoretinal morphology, anatomy, and pathology by clinical examination, imaging, and SD OCT.

Results—Linear and volumetric imaging was achieved with the handheld system in infant eyes despite tunica vasculosa lentis and vitreous bands. Imaging was not possible in eyes with notable vitreous hemorrhage. Analysis of SD OCT images revealed preretinal structures (ranging from 409 to 2700 μm in width and 212 to 440 μm in height), retinoschisis, and retinal detachment in the posterior pole of patients with advanced ROP. Both the retinoschisis and the preretinal structures were not identified on conventional examination or imaging by expert pediatric ophthalmologists. The preretinal structures varied in location and size, and may represent preretinal fibrovascular proliferation. Some were found in close proximity to blood vessels, whereas others were near the optic nerve.

Correspondence: Cynthia A. Toth, MD, Duke University Eye Center, PO Box 3802, Durham, NC 27710. cynthia.toth@duke.edu.

Financial Disclosure(s):
The author(s) have made the following disclosure(s):

Dr. Toth receives research support through Duke University from Alcon Laboratories, Bioptigen, Genentech, National Institutes of Health, North Carolina Biotechnology Center, and Sirion; is a consultant for Alcon Laboratories and Genentech; and receives royalties for ophthalmic surgical technologies through a Duke University agreement with Alcon. Drs. Toth and Farsiu have a patent pending on OCT image processing techniques. Dr. Farsiu receives research support through Duke University from Bioptigen. Dr. Joseph Izatt, who is principal investigator on National Institutes of Health grant R21EY017393 and co-investigator on North Carolina Biotechnology Center Collaborative Funding Grant 2007-CFG-8005 and Duke Translational Medicine Institute Subcontract 12 of National Institutes of Health Grant 5ULT-RR024128-03, has consulting, intellectual property, and equity relationships with Bioptigen, Inc.

Conclusions—Handheld SD OCT imaging can be performed on the sedated or nonsedated neonate and provides valuable subclinical anatomic information. This novel imaging modality can reveal the location and extent of posterior ROP pathology not evident on standard examination. This could affect future clinical decision-making if studies validate a management strategy based on findings from this imaging technique.

Despite advances in treatment, retinopathy of prematurity (ROP) is a major cause of vision loss in neonates.[1,2] This disease is characterized by an abnormal, premature arrest of developing retinal blood vessels. When this carefully orchestrated process is pathologically disrupted by premature birth, a subset of patients with ROP develop abnormal fibrovascular proliferation that can cause retinal detachment and permanent vision loss.

The Early Treatment of ROP study found that 9% of patients had an unfavorable anatomic outcome at 2 years despite laser ablation of high-risk eyes at prethreshold.[3] Prenner et al[4] showed that surgery for infants with stage 4 ROP without macula involvement is safe and may preserve the architecture of the macula leading to better visual outcomes. Similarly, Azuma et al[5] suggest that intervention with early vitreous surgery for aggressive posterior ROP may be indicated when laser ablation or cryotherapy does not prevent the progression to retinal detachment.[6] The ability to promptly recognize characteristics leading to active proliferation of fibrovascular tissue may lead to early intervention and better visual and anatomic outcomes.[7] The ability to recognize the early stage of retinal detachment is also important. In these studies, the extent of detachment and preretinal pathology was determined by ophthalmoscopic examination or review of fundus photographs.

Fundus examination with indirect ophthalmoscopy remains the gold standard for monitoring patients with ROP.[1,3,8] Fundus photography with computer-assisted tools is garnering interest to reduce the subjectivity of diagnosing plus disease.[9–11] However, new imaging technology is necessary to detect subclinical pathology that may improve our understanding of the underlying disease process and guide treatment decisions.

Optical coherence tomography (OCT) imaging has enhanced our understanding and treatment of adult macular diseases.[12] Positioning and cooperation requirements limit neonatal imaging with commercial tabletop OCT systems. A time-domain OCT (TD OCT) system recently was modified to image neonates with ROP in the operating room (OR).[13,14] Both of these studies demonstrated subclinical pathology, either retinoschisis or retinal detachment, in ROP. However, because of slow image acquisition, TD OCT requires an immobile eye for 1 or more seconds to avoid motion artifact. This limits the use of this device to anesthetized or sedated young patients.

The capability of performing in vivo high-resolution imaging would enhance our ability to detect, characterize, and follow ROP pathology. The higher capture rate of spectral domain optical coherence tomography (SD OCT), which is more than 40 times faster than TD OCT, diminishes motion artifact and makes handheld imaging possible.[15–17] Scott et al[16] demonstrated that a handheld SD OCT device can be used to image the retina in full-term infants with shaken baby syndrome. Chong et al[17] used the same system to image a young child with albinism. Both of these studies imaged infants under sedation or general anesthesia. In this study, we extend the application of OCT by using an SD OCT system that combines high-speed imaging and the use of a handheld probe, unavailable with existing TD OCT, to image the eyes of neonates with and without general anesthesia. We report the results of high-resolution, cross-sectional, and 3-dimensional SD OCT images in nonsedated and anesthetized neonates with advanced ROP.

Patients and Methods

Consent for this study was obtained as part of an approved study in accordance with the Duke University Health System Institutional Review Board. The patients included 3 infants with advanced ROP in both eyes. SD OCT imaging was performed in the neonatal intensive care unit (NICU) without sedation for 1 patient and in the OR under general anesthesia for 2 patients. We imaged all patients using a handheld SD OCT probe that replaced the conventional tabletop head on SD OCT systems (Bioptigen Inc., Research Triangle Park, NC). The handheld probe was connected by a flexible fiberoptic cable to the SD OCT system. For the third case, the original larger tabletop SD OCT system (same handheld probe) was switched to a more compact system on a moveable cart (Fig 1). All patients were supine during imaging. Both NICU and OR imaging were performed with continuous monitoring of vital signs. The NICU SD OCT imaging was performed on a nonintubated patient without sedation. A pacifier dipped with several drops of 24% sucrose solution (Toot Sweet, Hawaii Medical, Pembroke, MA) was orally administered during SD OCT imaging sessions in the NICU.[18]

In the NICU, SD OCT imaging was obtained 1 day before the next standard care clinical examination. Video-indirect ophthalmoscopy was performed at the time of the examination, but because those images were of limited quality as the result of poor focus, we used representative video-indirect images obtained 8 days after SD OCT imaging in the NICU for comparison in this study. Spectral domain optical coherence tomography imaging was performed in the NICU bed with a lid speculum and topical proparacaine anesthesia. The examiner held the noncontact hand-piece over the infant's eye, while resting her fingers on the face and wrists on the side of the bed to stabilize the probe. The visible light emitted from the handpiece into the patient's eye is a narrow, dim red light. There is no bright flash of light discharged during the examination.

In the OR, the examiner had the option of using a wrist rest to stabilize her hands while holding the SD OCT handpiece (Fig 1). Color fundus photographs were captured using contact Retcam imaging (Clarity Medical Systems, Pleasanton, CA) with methyl-cellulose gel on the cornea.

Analysis and capture of SD OCT images were performed in a manner similar to the protocol described by Scott et al.[16] Briefly, SD OCT images were captured using Bioptigen software version 1755. The software allowed the user to set up length, orientation (0 –360 degrees), number of A-scans per B-scan, and B-scans per volumetric scan, as desired. For this study, our group defined linear scans as multiple B-scans of the same characteristics captured from the same retinal location, volumetric-rectangular scans as multiple B-scans stepped across a rectangular area of the retina, and mixed scans as low-resolution volumetric scans with higher-resolution linear scans at the center line of the rectangle. Qualitative image processing of the acquired scans were performed using the Duke Optical Coherence Tomography Retinal Analysis Program.[19] Adobe Photoshop Creative Suite 3 (Adobe Inc., San Jose, CA), and ImageJ (National Institutes of Health, Bethesda, MD) software programs were used for image visualization, enhancement, and annotation of structures observed on cross-sectional SD OCT scans.[15] Three-dimensional videos and composite images were created using AMIRA version 4.1 software (Visage Imaging Inc., Carlsbad, CA). Duke Optical Coherence Tomography Retinal Analysis Program was also used to create an adaptive, contrast-enhanced, summed voxel projection (SVP) 2-dimensional image analogous to a fundus photograph created by axially collapsing B-scans.[20] The anatomic findings visible on Retcam, video-indirect images, and clinical examination notes were compared with SD OCT images. All SD OCT scans were evaluated, and interpretable scans from each study were used for analysis.

Case Reports and Results

Case 1

A former 650-g, 23-week postmenstrual age (PMA), Caucasian twin male received confluent laser to both eyes at 32 weeks PMA by an experienced pediatric ophthalmologist. The patient had aggressive posterior ROP, zone I with severely immature retinal development and plus disease.[6] At 37 weeks PMA, clinical examination with indirect ophthalmoscopy revealed zone I ROP with immature tortuous vessels in 4 quadrants in both eyes and suspicion of intraretinal neovascularization in the left eye. Confluent chorioretinal scars were noted for 360 degrees in both eyes without skip areas. There was no evidence of fibrovascular organization, retinoschisis, vitreous hemorrhage, or retinal detachment.

Handheld SD OCT imaging was performed without sedation in both eyes within 24 hours of the clinical examination (Fig 1). Spectral domain optical coherence tomography images revealed clinically undetected preretinal structures and retinoschisis in both eyes and a very shallow retinal detachment in the left eye (Fig 2F). Multiple, well-demarcated preretinal structures were frequently located adjacent to and over blood vessels in the right eye (Fig 3B, C) and over or adjacent to the optic nerve in the left eye (Fig 2C, D). These preretinal structures were hyper-reflective and caused a shadowing artifact (Figs 2D and 3C). There was prominent focal shadowing within localized areas of the preretinal structure (Fig 2D, F).

The preretinal structures in each of the cross-sectional scans were manually delineated (by author RM), and from this series of scans an SVP image was developed projecting the structures relative to the vessel pattern in the posterior pole (Figs 2 and 3; Video 1, available at http://aaojournal.org).[15] Although the lateral dimension of these lesions varied from a minimum of 409 μm to a maximum of 2.7 mm in any horizontal scan, the height of the lesions did not vary much from lesion to lesion and was approximately (212– 440 μm) (Figs 2D, F and 3C).

Video-indirect ophthalmoscopic images obtained 8 days after SD OCT imaging (Figs 2A and 3A) revealed immature, tortuous retinal vasculature in both eyes with persistent neovascularization behind the laser margin in the left eye. There was no evidence of preretinal tissue overlying the retina, retinal detachment, or retinoschisis in either eye.

Nine weeks after laser treatment, the patient developed bilateral stage 4 retinal detachments (Figs 2G and 3D). During a preoperative examination under anesthesia (EUA), preretinal white tissue was observed overlying the macula in both eyes on indirect ophthalmoscopy (Figs 2G and 3D). The patient underwent lens-sparing vitrectomy with posterior hyaloid and preretinal membrane removal in each eye.

Case 2

A former 750-g, 24-week PMA, Caucasian male infant was referred for diode laser treatment of both eyes at 38 weeks. One week after laser, an EUA was performed. Portable slit-lamp examination revealed engorged persistent tunica vasculosa lentis in both eyes. Indirect ophthalmoscopy demonstrated 4 quadrants of plus disease in both eyes, stage 4A in the right eye, and stage 4B in the left eye. There was a persistent hyaloidal stalk that emanated from the optic nerve to the lens in both eyes. The optic nerve appeared to be hypoplastic in the right eye. Retcam fundus photography demonstrated similar findings to indirect ophthalmoscopy.

Spectral domain optical coherence tomography imaging at the time of EUA revealed retinal detachment, preretinal structures, and retinoschisis in the right eye. Spectral domain optical coherence tomography was not attempted in the left eye because of persistent fetal

vasculature obstructing the view to the retina. Spectral domain optical coherence tomography imaging in the right eye revealed retinal detachment in areas where clinically visible retinal detachment was observed (Fig 4A, D). Spectral domain optical coherence tomography imaging of the posterior pole also revealed the posterior extent of retinal detachment in areas that were not clinically observed (i.e., potentially 4B rather than 4A detachment) (Fig 4B, C). Retinoschisis was present in areas of clinically detached and attached retina (Fig 4B, D). The vascular pattern including extent of tortuousity was visible on the SVP image and correlated well with the vascular pattern on the Retcam fundus photograph as seen in Figure 4A and C.

A mechanical vitrectomy with membrane peeling was performed at the time of EUA for stage 4B retinal detachment in the left eye. One week later, another EUA was performed in the OR and SD OCT imaging was performed on the right eye. Image quality was worse than on previous examination because of posterior synechiae causing poor pupillary dilation and persistent fetal vasculature. Vitrectomy surgery was performed in the right eye for the retinal detachment.

Case 3

A former 650-g, 23-week PMA, Caucasian male was evaluated for progressive ROP despite laser photocoagulation in both eyes. At 37 weeks PMA, he had lens sparing vitrectomy in the left eye for a stage 4A detachment. Four days later, he had an EUA with bilateral SD OCT imaging before lens sparing vitrectomy in the right eye. Clinical examination revealed persistent tunica vasculosa lentis in both eyes, zone 1, stage 4B detachment in the right eye with vitreous hemorrhage and a dense tractional membrane extending in a plaque across the macula to the optic nerve (Fig 5A), and residual focal tractional retinal detachment temporally in the left eye without hemorrhage.

On SD OCT imaging of the right eye, we found retinoschisis, dense preretinal membranes with traction, massive retinal thickening (>1000 μm) and distortion of the macular region, and preretinal and intraretinal hyperreflective dots (Fig 5C, D). Sub-retinal structures with foci of hyperreflective dots were also observed (Fig 5D). The vascular pattern could be detected (Fig 5B) on SD OCT but could not be correlated to the color fundus photograph (Fig 5A) because of poor image quality from vitreous hemorrhage. In the left eye, there was persistent focal subretinal fluid, retinoschisis, and subretinal hyperreflective dots (Fig 6A).

The pathology evident by SD OCT imaging is summarized in Table 1. Of note, although scans were performed across the presumed location of the fovea in all patients, foveal contour was not appreciated in any images. This is consistent with histopathologic studies that show foveal contour is first appreciated at approximately 40 weeks PMA.[21,22]

Discussion

We report the use of a handheld SD OCT device to image premature neonates with ROP without sedation at the bedside and under general anesthesia in the OR. We demonstrate the ability of SD OCT to evaluate subclinical pathology such as preretinal structures, retinoschisis, and retinal detachment in patients with advanced ROP. Until now, OCT imaging of neonates or infants required patients to be under anesthesia to limit head and eye motion. The fast acquisition time, along with a maneuverable cart system with handheld scanning head, made it possible to image at one neonate's bedside rather than under anesthesia. In this study, handheld SD OCT produced clinically useful images both at the bedside and in the OR in premature infants with advanced ROP.

The ability to image premature infants, without the risk of general anesthesia, overcomes a major hurdle in pediatric retinal imaging. Although the use of a few drops of oral 24% sucrose solution administered on a pacifier to diminish stress during imaging seemed to diminish some patient movement, the motion produced by infant sucking remains visible on the SVP images (Figs 2B and 3B). Methylcellulose or balanced salt solution was initially used to lubricate the cornea for SD OCT imaging in 2 patients, but liquid gel artificial tears improved image quality in patient 3. Further study will be helpful to evaluate and refine the utility of this system for nonanesthetized neonatal retinal imaging.

The striking size and extent of preretinal structures revealed with SD OCT imaging in the advanced ROP eye is a salient finding of this study. The precise makeup of this tissue is unknown and requires histopathologic or angiographic correlation. We note that some of these structures caused variable or incomplete shadowing for the length of the structure (Fig 2D, F). This suggests that the tissue's composition is heterogeneous, and vessels within the structures may cause shadowing. In addition, the preretinal structures were often in close proximity to blood vessels (Fig 3B). There was subsequent preretinal fibrous tissue in these areas at the time of retinal detachment surgery. We believe that these preretinal structures are fibrovascular and likely similar to neovascular tufts that have been found to be associated with disease progression in cases of zone II ROP.[23]

We hypothesize that preretinal structures may represent remnants of the hyaloidal vasculature or abnormal retinal vascular development. The hyaloidal vasculature undergoes apoptosis at 28 to 30 weeks PMA.[24] Because all of our patients were born at approximately 24 weeks PMA, peripapillary preretinal structures may consist of hyaloidal remnants. Preretinal structures near blood vessels may represent abnormal vascular development. Recent insight into vascular biology suggests that zone I, unlike zones II and III, may represent an abnormal arrest of vasculogenesis, de novo formation of blood vessels from vascular precursor cells.[25] We believe that the preretinal structures observed on SD OCT in advanced ROP may represent abnormal vasculogenesis or incomplete regression of the hyaloid. The images in case 1 were captured weeks after laser therapy, and although vitreous or fibrous organization was not visible, there may have been hyaloid contracture as described by Joshi et al[26] or vitreous organization as described by Coats.[27] We hypothesize that in this posterior location, this may occur at sites of preretinal vascular abnormalities.

Coats[27] recognized the potential for unrecognized subclinical detachment of the fovea in temporal retinal detachment in ROP. Subclinical foveal detachment that is unrecognized on ophthalmoscopic examination might explain poor visual outcomes in some stage 4A eyes, because intervention in the stage 4A eye has been correlated with improved visual outcomes in ROP compared with stage 4B or 5 eyes.[4] In this study, SD OCT imaging detected subclinical macular retinal detachment. Patient 2 demonstrated clinically overt retinal detachment in the periphery, but the macula appeared to be attached on indirect ophthalmoscopy and Retcam photography (Fig 4A). Spectral domain optical coherence tomography imaging of the posterior pole (Fig 4B, C) revealed a shallow retinal detachment across the presumed area of the macula that was not clinically appreciated. Spectral domain optical coherence tomography may be beneficial in detecting subclinical macular retinal detachment and may guide surgical decision-making. Spectral domain optical coherence tomography may illustrate subclinical pathology and be a potential strength in ROP screening in the NICU. First, however, studies are needed to evaluate potential management strategies based on findings from this imaging technique.

Consistent with previous studies using TD OCT in stage 4 ROP,[14] all of our patients demonstrated a retinoschisis-like appearance of the retina (Figs 2, 4 – 6), none of which was visible on clinical examination. In some areas this appeared as a splitting of the more highly

reflective inner retinal layers (Figs 4B, 5C, and 6A) associated with vitreous attachment and upward tenting of the retina (Fig 5C), whereas in other areas this involved deeper retinal layers with a “lamellar schisis-like change” similar to that described by Joshi et al[14] (Figs 2F and 4D; Video 2, available at http://aaojournal.org). From this limited study, we cannot definitively differentiate traction-associated schisis from abnormal foveal development or diffuse cystoid macular edema. In patients 2 and 3, the subclinical retinoschisis (Figs 4B and 5D) was associated with clinically visible tractional detachment of the retina (Figs 4A and 5A). In patient 1, subclinical retinoschisis and retinal detachment occurred before the appearance of fibrovascular organization of the vitreous or stage 4 ROP in the left eye (Fig 3F).[28] He subsequently progressed to clinically evident tractional retinal detachments within 4 weeks (Figs 2G and 3D) of this examination. We hypothesize that some subclinical retinoschisis may result from traction associated with fibrovascular organization and may serve as a harbinger for tractional retinal detachment. In diabetes, tractional elevations of the retina have been associated with either retinoschisis or retinal detachment.[29] In accordance with Joshi et al,[14] we believe that poor visual outcomes after surgical intervention in advanced ROP may be partially explained by undiagnosed lamellar schisis-like retinal changes at the time of intervention.[30] Future study is required to determine whether detecting subclinical retinoschisis by SD OCT will help predict visual outcomes.

Major limitations of this study include the small number of patients, motion artifact in images from the nonsedated subject, and adjustment of the system for the premature infant eye. These issues are being addressed in a prospective NICU study with recruitment of a larger number of patients with different stages of ROP. An experienced operator was necessary to use the handheld SD OCT probe to account for motion artifact from hand movement and patient motion. These artifacts can cause abnormal or complete loss of B-scans requiring careful attention during analysis (Fig 2B, white arrows). Because of the shorter axial length of the premature infant eye, the projected imaging area was smaller than predicted by scan settings for the adult. Also, a clipping effect was produced by the pupil on the B-scans because we used a standard adult reference arm length for the SD OCT system (black margins on the right side of the images in Fig 4B). We are working to correct these 2 issues in future studies by adjusting scan length for the horizontal magnification of the infant eye and modifying the reference arm for the axial length of the neonatal eye. The maximum extent of peripheral imaging was not assessed in this pilot study, which focused on posterior pole pathology in advanced ROP. Ongoing studies of SD OCT imaging in zone II ROP will assess the feasibility and limitations of imaging peripheral pathology.

In conclusion, this proof-of-principal study represents the first use of SD OCT in a nonsedated patient with ROP and demonstrates that it may be possible to overcome the major hurdle of the risk of anesthesia in neonatal retinal imaging. Moreover, in patients with advanced ROP, we demonstrate the utility of SD OCT imaging in subclinical preretinal, intraretinal, and subretinal pathology that is likely to affect the precision of our assessment of the extent of disease. We believe that analysis of SD OCT images in eyes with ROP will provide insight into the pathogenesis of ROP. More work is needed to determine the frequency and predictive value of these findings in patients with ROP.

Acknowledgments

Dr. Joseph Izatt provided essential input for optimizing the SD OCT system imaging in the infant eye.

Supported by Angelica and Euan Baird, North Carolina Biotechnology Center Collaborative Funding Grant 2007-CFG-8005, National Institutes of Health R21 EY017393, and the Duke Translational Medicine Institute Subcontract 12 of National Institutes of Health Grant 5ULT-RR024128-03.

References

1. Tasman W. Multicenter trial of cryotherapy for retinopathy of prematurity. Arch Ophthalmol. 1988; 106:463– 4. [PubMed: 3281639]
2. Early Treatment for Retinopathy of Prematurity Cooperative Group. Revised indications for the treatment of retinopathy of prematurity: results of the Early Treatment for Retinopathy of Prematurity randomized trial. Arch Ophthalmol. 2003; 121:1684–94. [PubMed: 14662586]
3. Early Treatment for Retinopathy of Prematurity Cooperative Group. The Early Treatment for Retinopathy Of Prematurity Study: structural findings at age 2 years. Br J Ophthalmol. 2006; 90:1378– 82. [PubMed: 16914473]
4. Prenner JL, Capone A Jr, Trese MT. Visual outcomes after lens-sparing vitrectomy for stage 4A retinopathy of prematurity. Ophthalmology. 2004; 111:2271–3. [PubMed: 15582085]
5. Azuma N, Ishikawa K, Hama Y, et al. Early vitreous surgery for aggressive posterior retinopathy of prematurity. Am J Ophthalmol. 2006; 142:636– 43. [PubMed: 17011857]
6. International Committee for the Classification of Retinopathy of Prematurity. The International Classification of Retinopathy of Prematurity revisited. Arch Ophthalmol. 2005; 123:991–9. [PubMed: 16009843]
7. Coats DK, Miller AM, Hussein MA, et al. Involution of retinopathy of prematurity after laser treatment: factors associated with development of retinal detachment. Am J Ophthalmol. 2005; 140:214–22. [PubMed: 16086945]
8. Committee for the Classification of Retinopathy of Prematurity. An international classification of retinopathy of prematurity. Arch Ophthalmol. 1984; 102:1130– 4. [PubMed: 6547831]
9. Wilson CM, Cocker KD, Moseley MJ, et al. Computerized analysis of retinal vessel width and tortuosity in premature infants. Invest Ophthalmol Vis Sci. 2008; 49:3577– 85. [PubMed: 18408177]
10. Wallace DK, Freedman SF, Zhao Z, Jung SH. Accuracy of ROPtool vs individual examiners in assessing retinal vascular tortuosity. Arch Ophthalmol. 2007; 125:1523–30. [PubMed: 17998514]
11. Chiang MF, Gelman R, Williams SL, et al. Plus disease in retinopathy of prematurity: development of composite images by quantification of expert opinion. Invest Ophthalmol Vis Sci. 2008; 49:4064–70. [PubMed: 18408188]
12. Huang D, Swanson EA, Lin CP, et al. Optical coherence tomography. Science. 1991; 254:1178–81. [PubMed: 1957169]
13. Patel CK. Optical coherence tomography in the management of acute retinopathy of prematurity. Am J Ophthalmol. 2006; 141:582– 4. [PubMed: 16490519]
14. Joshi MM, Trese MT, Capone A Jr. Optical coherence tomography findings in stage 4A retinopathy of prematurity: a theory for visual variability. Ophthalmology. 2006; 113:657– 60. [PubMed: 16581425]
15. Stopa M, Bower BA, Davies E, et al. Correlation of pathologic features in spectral domain optical coherence tomography with conventional retinal studies. Retina. 2008; 28:298–308. [PubMed: 18301035]
16. Scott AW, Farsiu S, Enyedi LB, et al. Imaging the infant retina with hand-held spectral-domain optical coherence tomography. Am J Ophthalmol. 2009; 147:364–73. [PubMed: 18848317]
17. Chong GT, Farsiu S, Freedman SF, et al. Abnormal foveal morphology in ocular albinism imaged with spectral domain optical coherence tomography. Arch Ophthalmol. 2009; 127:37–44. [PubMed: 19139336]
18. Gal P, Kissling GE, Young WO, et al. Efficacy of sucrose to reduce pain in premature infants during eye examinations for retinopathy of prematurity. Ann Pharmacother. 2005; 39:1029–33. [PubMed: 15855243]
19. Farsiu S, Chiu SJ, Izatt JA, Toth CA. Fast detection and segmentation of drusen in retinal optical coherence tomography images. Proc SPIE. 2008; 6844:68440D.
20. Jiao S, Knighton R, Huang X, et al. Simultaneous acquisition of sectional and fundus ophthalmic images with spectral-domain optical coherence tomography. Opt Express [serial online]. 2005; 13:444–52. Available at: http://www.opticsinfobase.org/oe/abstract.cfm?uri=oe-13-2-444.

21. Hendrickson AE, Yuodelis C. The morphological development of the human fovea. Ophthalmology. 1984; 91:603–12. [PubMed: 6462623]
22. Yuodelis C, Hendrickson A. A qualitative and quantitative analysis of the human fovea during development. Vision Res. 1986; 26:847–55. [PubMed: 3750868]
23. Wallace DK, Kylstra JA, Greenman DB, Freedman SF. Significance of isolated neovascular tufts ("popcorn") in retinopathy of prematurity. J AAPOS. 1998; 2:52– 6. [PubMed: 10532368]
24. Eller AW, Jabbour NM, Hirose T, Schepens CL. Retinopathy of prematurity: the association of a persistent hyaloid artery. Ophthalmology. 1987; 94:444– 8. [PubMed: 2438623]
25. Flynn JT, Chan-Ling T. Retinopathy of prematurity: two distinct mechanisms that underlie zone 1 and zone 2 disease. Am J Ophthalmol. 2006; 142:46–59. [PubMed: 16815250]
26. Joshi MM, Ciaccia S, Trese MT, Capone A. Posterior hyaloid contracture in pediatric vitreoretinopathies. Retina. 2006; 26 (suppl):S38– 41. [PubMed: 16946676]
27. Coats DK. Retinopathy of prematurity: involution, factors predisposing to retinal detachment, and expected utility of preemptive surgical reintervention. Trans Am Ophthalmol Soc. 2005; 103:281–312. [PubMed: 17057808]
28. Hartnett ME, McColm JR. Fibrovascular organization in the vitreous following laser for ROP: implications for prognosis. Retina. 2006; 26(suppl):S24–31. [PubMed: 16946674]
29. Lincoff H, Serag Y, Chang S, et al. Tractional elevations of the retina in patients with diabetes. Am J Ophthalmol. 1992; 113:235– 42. [PubMed: 1543216]
30. Prenner JL, Capone A Jr, Ciaccia S, et al. Congenital X-linked retinoschisis classification system. Retina. 2006; 26(suppl):S61–4. [PubMed: 16946682]

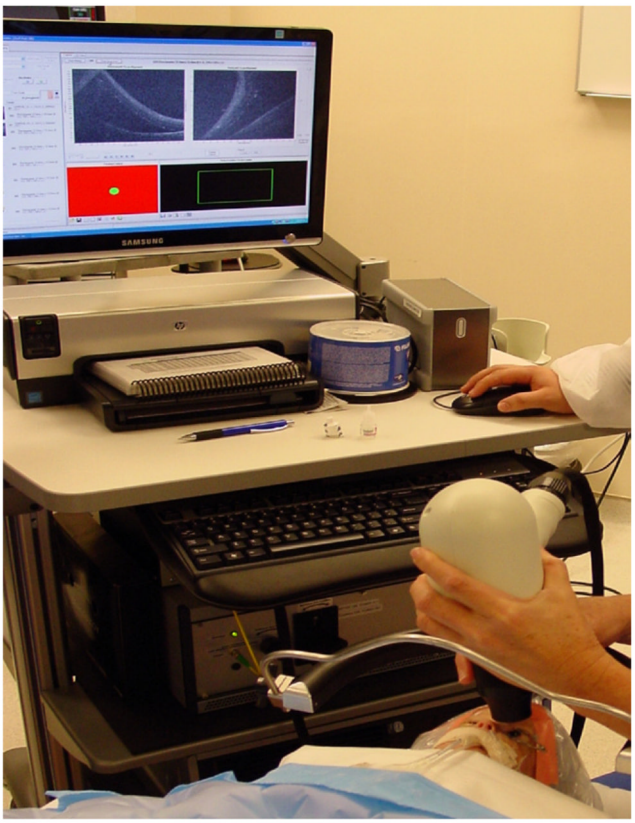

Figure 1.
Mobile workstation connected to a handheld probe for spectral domain optical coherence tomography (SD OCT) imaging in the operating room. A neonate is positioned in the supine position with the operator using a wrist rest to stabilize the noncontact hand-held SD OCT probe.

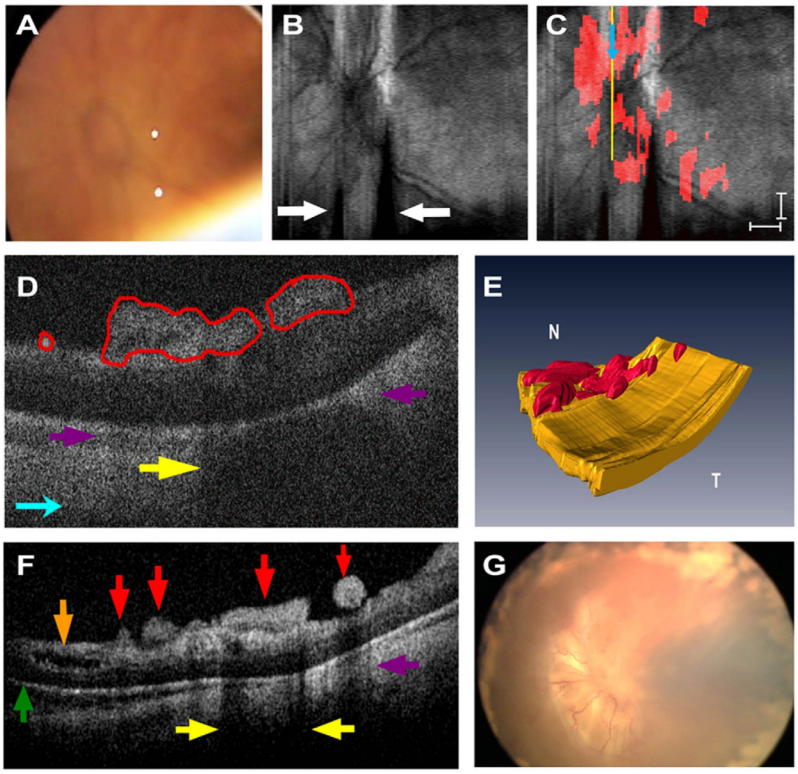

Figure 2.

Patient 1's left eye. **A**, Video-indirect image of the optic nerve and posterior pole of the retina without evidence of preretinal structures. **B**, Sum voxel projection image of optic nerve and posterior pole. There is also partial loss of some B-scan images from motion artifact (*white arrows*). **C**, Same summed voxel projection image in (**B**) with preretinal tissue (red areas in **D**) surrounding and overlying optic nerve. *Light blue arrows* provide image orientation (**B**, **C**). Scale bars are 1000 μm. **D**, Cropped cross-sectional spectral domain optical coherence tomography (SD OCT) image demonstrates preretinal structures traced in red and corresponds to yellow vertical line in (**C**). *Purple arrows* denote shadowing artifact of preretinal structures (**D**, **F**), and *yellow arrows* point to focal shadowing (**D**, **F**). **E**, Three-dimensional SD OCT image depicts preretinal structures in the posterior pole. N = nasal; T = temporal. **F**, Representative cross-sectional image demonstrates a variety of subclinical pathology. *Green arrow* indicates retinal detachment, *brown arrow* denotes retinoschisis, and *red arrows* point to preretinal structures. **G**, Retcam fundus photograph demonstrates tractional retinal detachment 1 month after SD OCT imaging.

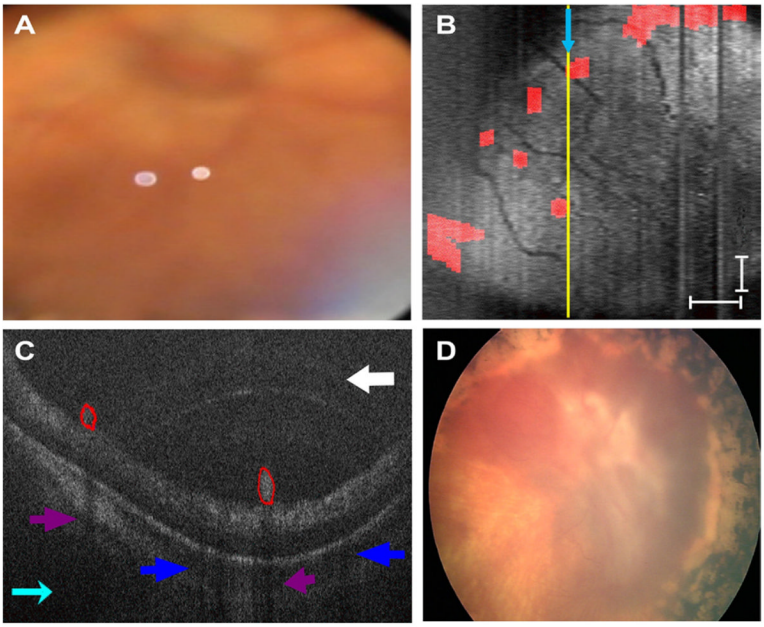

Figure 3.

Patient 1's right eye. **A**, Representative video-indirect ophthalmoscopy image without evidence of preretinal tufts and clear optic nerve head margins. **B**, Sum voxel projection of the preretinal tissue (red areas in **C**) demonstrates close proximity of preretinal structures to blood vessels. The *yellow line* corresponds to the location of the cross-sectional spectral domain optical coherence tomography (SD OCT) image in (**C**). *Light blue arrows* provide image orientation (**B**, **C**). Scale bars are 1000 μm. **C**, Cross-sectional SD OCT image demonstrates preretinal structures outlined in red. *White arrow* points to an arcing imaging artifact, *dark blue arrows* correspond to shadowing from retinal blood vessels, and *purple arrows* correspond to shadowing from preretinal structures. **D**, Retcam fundus photograph demonstrates tractional retinal detachment with dense pre-retinal fibrosis over the optic nerve and macula 1 month after SD OCT imaging.

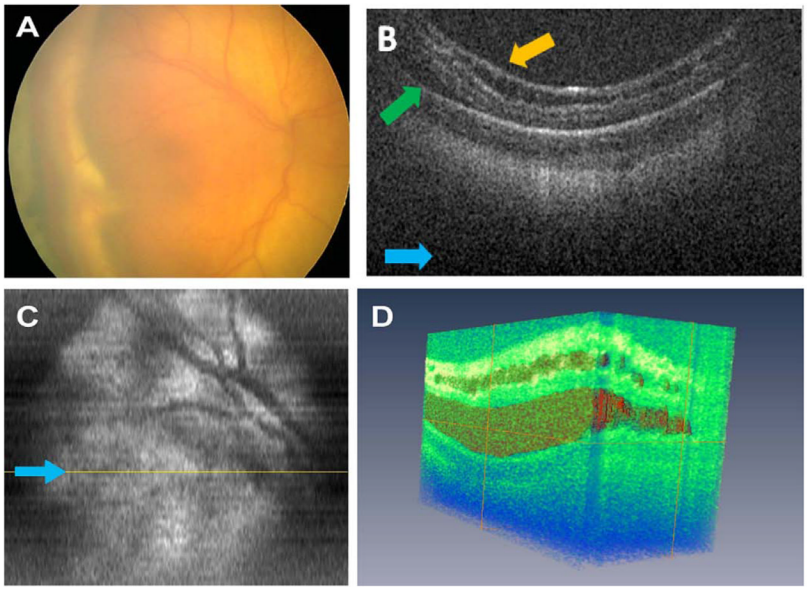

Figure 4.

Patient 2's right eye. **A**, Retcam fundus photography demonstrates tractional retinal detachment temporal to the fovea and chorioretinal scars from laser retinopexy. **B**, Cross-sectional spectral domain optical coherence tomography (SD OCT) image shows retinal detachment (*green arrow*) and subclinical retinoschisis (lamellar schisis) (*brown arrow*). *Light blue arrows* provide image orientation (**B**, **C**). **C**, Sum voxel projection image with yellow line corresponding to cross-sectional SD OCT image in (**B**). Vascular pattern can be correlated with image in (**A**). **D**, Three-dimensional SD OCT image from temporal side of retina depicts retinoschisis and retinal detachment.

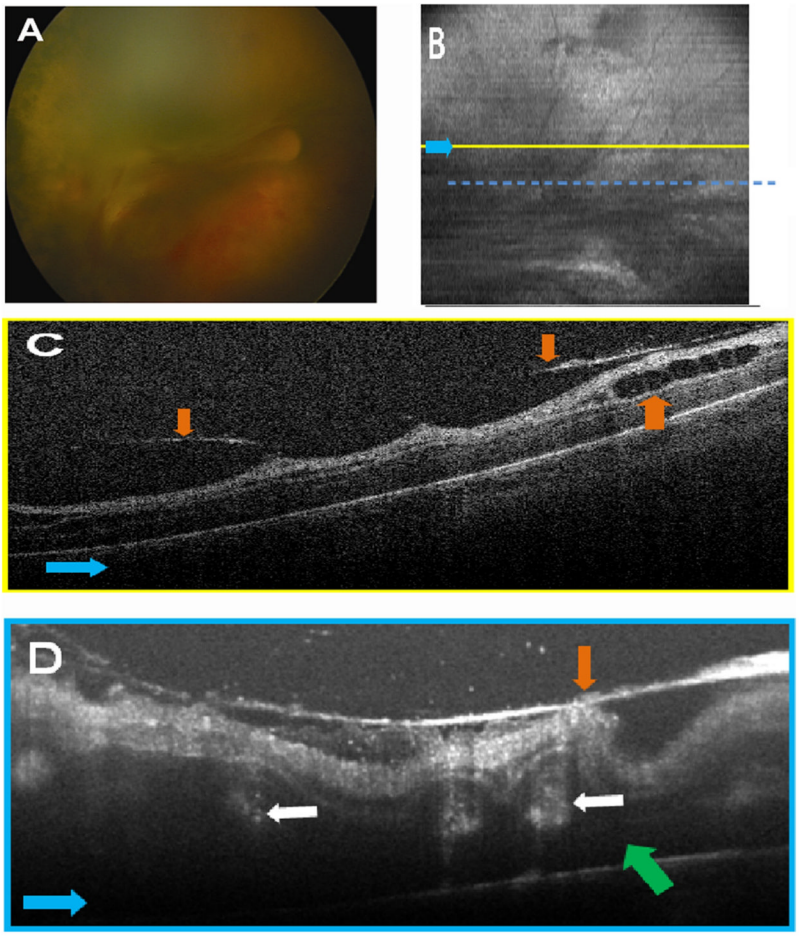

Figure 5.

Patient 3's right eye before vitrectomy surgery. **A**, Retcam fundus photography demonstrates tractional retinal detachment, vitreous hemorrhage, thick membrane complex over the macula creating prominent retinal folds, and tractional retinal detachment. **B**, Sum voxel projection with visible vascular pattern not seen clearly in (**A**). *Yellow line* corresponds to exact location of cross-sectional B scan in (**C**), and *dashed blue line* corresponds to approximate location of repeated linear scan in (**D**). Note that *dashed blue line* is partially displaced to the right of the image based on image alignment of this compared with the B scans comprising summed voxel projection in (**B**). *Light blue arrows* provide image orientation (**B–D**). **C**, Cross-sectional volumetric spectral domain optical coherence tomography (SD OCT) image shows vitreous attachments (*orange arrows* **C**, **D**) and retinoschisis (*brown arrow*). **D**, Cross-sectional summed linear SD OCT image shows retinal detachment (*green arrow*), epiretinal membrane with vitreous attachments, and deep intraretinal/subretinal structures (2 of 5 are labeled with *tan arrows*).

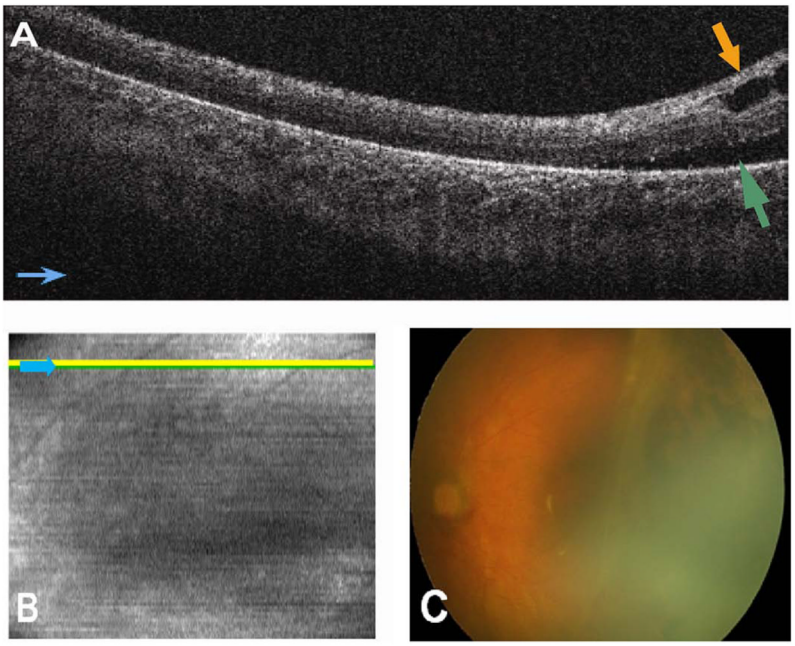

Figure 6.

Patient 3's left eye 4 days after vitrectomy surgery. **A**, Cross-sectional spectral domain optical coherence tomography (SD OCT) image demonstrates retinal detachment (*green arrow*) and retinoschisis (*brown arrow*). There are also subretinal hyperreflective dots present near *green arrow. Light blue arrows* provide image orientation (**A**, **B**). **B**, Sum voxel projection image with *yellow line* corresponds to the approximate location of the cross-sectional SD OCT image in (**A**). **C**, Retcam fundus photography demonstrates tractional retinal detachment and chorioretinal scars from laser retinopexy.

Table 1

Summary of Spectral Domain Optical Coherence Tomography Pathology

	Demonstrated in Figures
Vitreomacular traction	5
Epiretinal membrane	5
Preretinal presumed fibrovascular structures	2, 3
Intraretinal hyperreflective dots	4, 5
Retinal cysts	5
Retinoschisis	3–6
Retinal detachment	3–6
Subretinal hyperreflective structures	5, 6